Journal of Non-Crystalline Solids 489 (2018) 45–49

Contents lists available at ScienceDirect

Journal of Non-Crystalline Solids

journal homepage: www.elsevier.com/locate/jnoncrysol

Compositional dependence of physical and structural properties in $(Ge_{1-x}Ga_x)S_2$ chalcogenide glasses

Erwei Zhu, Xuhao Zhao, Jingsong Wang, Changgui Lin*

Laboratory of Infrared Materials and Devices, Research Institute of Advanced Technology, Ningbo University, Ningbo 315211, China
Key Laboratory of Photoelectric Detection Materials and Devices of Zhejiang Province, Ningbo, 315211, China

ARTICLE INFO

Keywords:
Chalcogenide glass
Raman spectra
Structure
Glass transition temperature
Hardness

ABSTRACT

Glassy and partially crystallized samples of $(Ge_{1-x}Ga_x)S_2$ (0 mol% ≤ x ≤ 50 mol%) were prepared and investigated for the Ga effect on their physical and structural properties. For low Ga content (0 mol% ≤ x ≤ 30 mol%), homogeneous glassy samples were prepared and present good physical properties, such as high glass transition temperature (> 400 °C) and Vickers hardness (> 2.60 GPa). With the Ga substitution for Ge, the thermal stability of samples decreases, leading to the precipitation of α-Ga_2S_3 crystallites when x > 40 mol%. Structural evolution of $(Ge_{1-x}Ga_x)S_2$ samples was investigated by Raman spectra and X-ray diffraction techniques. The correlation between the physical properties and structural evolution was established.

1. Introduction

Chalcogenide glasses attract increasing attentions because of their intriguing properties [1], including low phonon energy [2,3], wide transmission range extending to mid-infrared (IR) [4], high refractive index [5], high optical nonlinearity [6,7], photosensitivity [8], fast ionic conductivity [9], ease of fabrication and processing, and good chemical durability [10]. Chalcogenide glasses are currently recognized as promising materials for a variety of photonic applications, such as ultrafast all-optical switch [6,11], frequency converter [12], optical amplifier [13], IR fiber and fiber laser [8]. Among the numerous research reports of chalcogenide glasses, including sulfide, selenide, and telluride glasses, Ge-S-based glass is one of the most frequently investigated glass matrices because of its good visible transparency, excellent glass-forming ability, superior mechanical properties, and preferable thermal and chemical stabilities. Furthermore, the incorporation of other metallic elements, e.g. gallium and indium, endows Ge-S-based glasses favorable properties including high rare-earth [14,15] and alkali halide solubility [16–18], flexibility to be processed in the forms of fiber and film [19,20], and controllable crystallization [17,18,21–23]. Thus, chalcogenide glasses of Ge-X-S (X = Ga, In, etc.) have been extensively investigated from the aspects of glass-forming region, physical properties, and network structure.

The incorporation of Ga into Ge-S-based glasses results in high glass transition temperature (T_g), high rare-earth ions and alkali halides solubility, and good transparency in the visible that permitting a broad range of excitation wavelengths. The features of Ge-Ga-S glasses allow preferable flexibility to tune their optical, electronic, thermal, mechanical and other physical properties through elaborated compositional design [15,18,23–28]. Gallium plays a positive role in promoting solubility of rare-earth ions and alkali halides, and controllable crystallization. This role is determined by the variation of glass network structure caused by Ga [28].

The structural response of gallium on the physical properties was investigated mostly along the stoichiometric ratio of GeS_2-Ga_2S_3 in glass-forming region [16,17,29]. In the case of stoichiometric compositions, the physical properties of GeS_2-Ga_2S_3 glasses have been demonstrated to be determined by the variation of [S_3Ga-GaS$_3$] units. For the Ge-Ga-S glasses with non-stoichiometric compositions, the effect of Ga addition on physical and structural properties has been discussed along the compositions of (1-x)$GeS_{2.5}$-xGa (0 mol% ≤ x ≤ 40 mol%) that ranging from S-rich to S-deficient regions [28]. Both [Ga(Ge)S_4] and [S_3Ga(Ge)-Ga(Ge)S_3] are formed in the Ge-Ga-S glasses. However, the competitive coordination between Ge and Ga with S has not been studied ever. Therefore, $(Ge_{1-x}Ga_x)S_2$ samples were chosen here to learn the effect of Ga substitution for Ge on the physical and structural properties and to clarify the competitive behavior between Ge and Ga.

2. Experimental

Glassy and partially-crystallized samples with the compositions of $(Ge_{1-x}Ga_x)S_2$ (0 mol% ≤ x ≤ 50 mol%) were prepared by conventional melt-quenching technique. GAx (x = 0, 10, 20, 30, 40, and 50) is designated as the abbreviation of these samples. About 12 g mixtures of

* Corresponding author.
E-mail address: linchanggui@nbu.edu.cn (C. Lin).

https://doi.org/10.1016/j.jnoncrysol.2018.03.030
Received 17 January 2018; Received in revised form 10 March 2018; Accepted 12 March 2018
0022-3093/ © 2018 Elsevier B.V. All rights reserved.

high purity reagents of Ge (5 N), Ga (5 N) and S (6 N) were weighed and loaded into quartz ampoules which were sealed subsequently under a vacuum of about 10^{-3} Pa. The ampoules of 9 mm inner diameter were shifted into a rocking furnace and heated slowly to 980 °C. After melting, quenching, and annealing, rod samples were obtained, and finally cut and polished into slices of 2 mm thickness.

Thermal analysis was performed by differential scanning calorimeter (DSC, TA Q2000, USA). Characteristic temperatures, including T_g, onset temperature of crystallization, T_x, and temperature of crystallization peak, T_p, were obtained by heating ~10 mg sample in a hermetic aluminum pan at 10 °C/min rate under N_2 atmosphere. Densities were measured at room temperature according to Archimedes' principle which consists in comparing the difference of sample weights in air and distilled water. Vickers hardness (H_v) was determined using a micro-hardness tester (Hengyi MH-3, Shanghai, China) with a charge of 100 g for 5 s. A series of ten measurements were carried out and averaged for each sample and the experimental error on H_v, resulting from the inaccuracy of the measurement of the half of the mean size of the two diagonals, was within ± 0.02 GPa. Visible and near-IR transmission spectra between 320 and 2500 nm were recorded using a spectrometer (PerkinElmer-LAMBDA 950 spectrophotometer). Mid-IR transmission spectra between 2.5 and 13 μm were recorded using FT-IR spectrometer (Nicolet 380 FT-IR Spectrometer).

X-ray diffraction (XRD) patterns were recorded by a diffractometer (D2 Phaser, Bruker, Germany) using CuKα radiation with a step width of 0.02°. Raman spectra were obtained using a Raman spectrometer (Renishaw InVia, England) equipped with a LD laser operating at 785 nm. The LD laser with a power < 50 mW was used as an excitation source for the avoidance of local laser damage. The resolution of the Raman spectra was 1 cm^{-1}. Micrographs of the fresh surfaces of as-prepared and etched by 2% NaOH solution for 20 s were recorded by using a scanning electronic microscope (SEM, Tescan VEGA 3SBH, Czech). The linear refractive indices of samples were measured as a function of wavelength by using IR variable angle spectroscopic ellipsometry (IR-VASE, J.A. Woollam Co., Lincoln, NE).

3. Results

Transmission spectra of the $(Ge_{1-x}Ga_x)S_2$ glassy and crystallized samples are present in Fig. 1. The inset photos show the effect of Ga substitution for Ge on their appearance, which agrees with the red shift of visible cut-off edge listed in Table 1. The decreasing of the maximum transmittance of GA40 and GA50 is due to the scattering loss caused by the precipitation of crystalline particles inside the glass matrices. As shown in Fig. 2, α-Ga_2S_3 particles were precipitated in the GA40 and GA50 samples. Although the diffraction peaks of G40 sample are feeble, crystalline particles precipitated in the center of sample discs can be observed clearly. It is worthy to note that the α-Ga_2S_3 phase (*P*61 space group, No. 169) here is different from that of *P*63*mc* group (No. 186) reported previously in GeS_2-Ga_2S_3 based glasses [21–23]. This phenomenon might be due to different crystallization pathways: the former is crystallized from $(Ge_{0.5}Ga_{0.5})S_2$ melt during melt-quenching process, whereas the latter is precipitated through the re-heating treatment of bulk glasses.

Fig. 3 displays the SEM micrographs of $Ge_{0.5}Ga_{0.5}S_2$ glass-ceramic sample. Needle-like crystalline phase can be observed as shown in Fig. 3a. The micrograph of the etched surface of $Ge_{0.5}Ga_{0.5}S_2$ glass-ceramic sample (Fig. 3b) exhibits the crystallites with the size of 5–10 μm. According to the XRD pattern in Fig. 2, this needle-like crystallites are belonging to α-Ga_2S_3 phase. Their big size is responsible for the decreasing of maximum transmittance and the red-shift of short wavelength cut-off edge at mid-IR region.

As listed in Table 1, the cut-off edge of short wavelength red-shifts as a function of Ga content. The density increases from 2.715 to 3.001 g/cm^3, and the Vickers hardness (H_v) decreases from 2.04 to 3.26 GPa. Fig. 4 shows the DSC curves of the $(Ge_{1-x}Ga_x)S_2$ (0 mol % ≤ x ≤ 50 mol%) samples and the T_g values are marked. Two obvious exothermic peaks are observed for GA30, GA40, and GA50 samples. The characteristic temperatures of T_g and T_x are marked in Fig. 4, and listed in Table 1. The value of T_g ranging from 520.4 °C to 387.1 °C decreases with increasing Ga content. The criterion ΔT ($\Delta T = T_x - T_g$), which is critical to analyze the thermal stability of a glass, decreased gradually with the addition of Ga. This decreasing thermal stability is due to the structural degradation of the formation of Ga—Ga metal bonds [10,23,30].

The refractive index (n) changes of $(Ge_{1-x}Ga_x)S_2$ (0 mol % ≤ x ≤ 40 mol%) samples as a function of wavelength following Cauchy dispersion formula are shown in Fig. 5. Because of the larger polarizability of Ga (8.12×10^{-24} cm^3) compared with that of Ge (6.07×10^{-24} cm^3), n value is in direct relation with glassy compositions and increases with increasing Ga content. The n value at 10 μm increases from 2.0129 (GA0) to 2.0455 (GA30). GA30 and GA40 have nearly the same refractive index dispersion within long wavelength region. This similar dispersion might be due to the partial precipitation of α-Ga_2S_3 phase in GA40, which leads to its Ga content in the residual glassy matrix akin to that of GA30. It is noted that the refractive indices are all relatively high, suggesting large nonlinear refractive indices of these glasses and also their potential applications in optoelectronic field.

To reveal the compositional trend of structural evolution, Raman spectra of $(Ge_{1-x}Ga_x)S_2$ (0 mol% ≤ x ≤ 50 mol%) samples were recorded as shown in Fig. 6. Raman spectrum of GeS_2 (GA0) in Fig. 6 is in

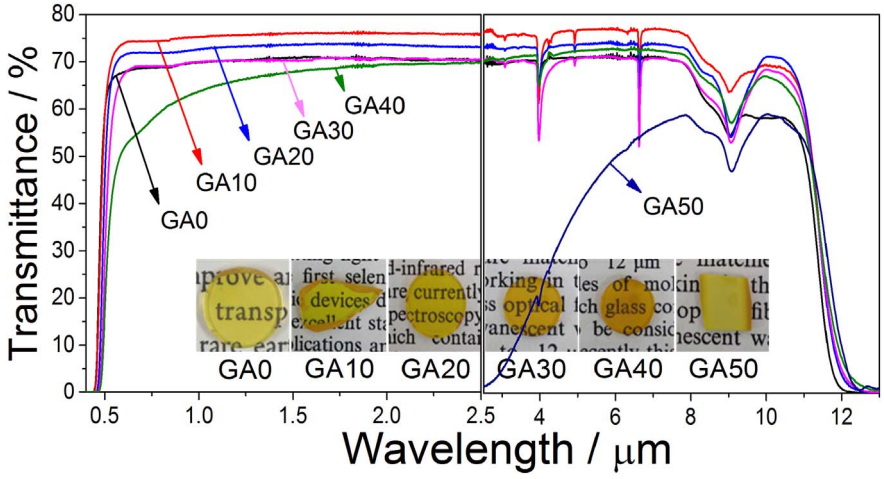

Fig. 1. Vis-near IR and mid-IR transmission spectra of $(Ge_{1-x}Ga_x)S_2$ (0 mol% ≤ x ≤ 50 mol%) samples. Inset represents the photos of as-prepared samples.

Download English Version:

https://daneshyari.com/en/article/7899979

Download Persian Version:

https://daneshyari.com/article/7899979

Daneshyari.com